Investigations on working principles and design methods for metamaterial silencers

Agostino Troll[1], Jens Rohlfing[1], Jan Küller[2], Georg Fischer[2], Daniel Beer[2] und Andreas Lühring[3]

[1]*Fraunhofer IBP, Nobelstraße 12 70569 Stuttgart*
[2]*Fraunhofer IDMT, Ehrenbergstr. 31, 98693 Ilmenau*
[3]*Fraunhofer IFAM, Wiener Straße 12, 28359 Bremen*
E-Mail: agostino.troll@ibp.fraunhofer.de

Introduction

Silencers are usually filled with porous material, as shown on the left hand side in Figure 1. When the sound wave travels through the porous silencer, friction losses occur inside the material, which reduces the particle velocity and hence sound pressure level.
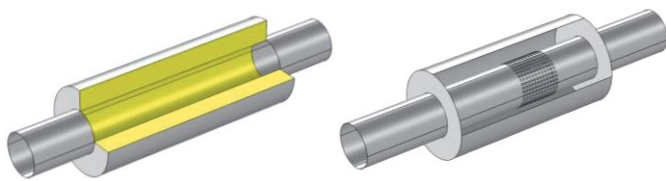

Figure 1: Porous (left) and resonant (right) silencers.

As indicated in Figure 2, typically porous silencers have a maximum in transmission loss around the mid audio frequency range. Towards higher frequencies, the effectiveness is limited by the dimension of the free cross-section. Towards low frequencies, the effectiveness is mainly limited by the acoustic absorption of the porous material layer.
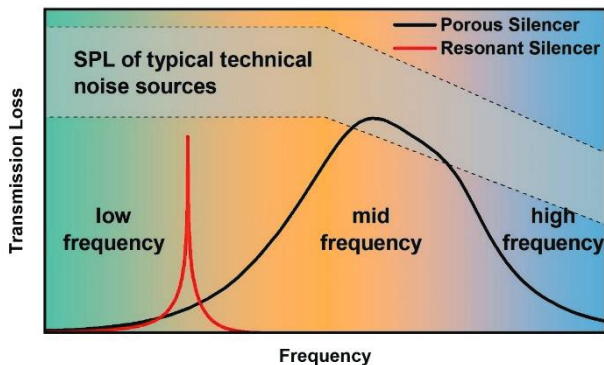

Figure 2: Typical transmission loss of porous and resonant silencers.

This is not ideal, since the sound emissions of typical sound sources, such as fans or motors, have significant low frequency components, as indicated by the shaded area in Figure 2. For this reason silencers based on porous material alone, are often not a suitable solution.

One way of making silencers more effective at low frequency range is to integrate acoustic resonators, as shown on the right hand side in Figure 1. However, to be effective at low frequencies acoustic resonators with a large volume are required. Hence, low frequency silencers available today feature only a small number of resonators or even only one acoustic resonator. They also tend to be bulky and can be expensive. A new approach to reduce low and mid audio frequency noise is that of acoustic metamaterials, based on arrays of acoustic resonators.

Metamaterials are artificial resonant structures, often based on a periodic sub structure, which combine local resonance effects with effects due to periodic spacing and geometric distribution. In noise control applications, this can be used to maximize absorption and reduce installation space. The essential question for silencers based on acoustic metamaterials are, if and how one single Resonator can be replaced by several resonators in order to reduce the required installation space and to increase the performance in terms of transmission loss at the same time.

In this paper, periodic resonator arrangements are discussed with respect to Bragg reflections and the propagation of Bloch waves in ducts.

Theory of Bloch waves in ducts

Bloch waves are waves, e.g. electromagnetic or mechanical, which move through a periodic potential. With this type of wave propagation special effects occur, which are discussed in this section for the case of one-dimensional acoustic waves. In ducts one-dimensional plane wave propagation occurs below the cut-on frequency. The description is based on Bloch's theorem, given by equation 1. Bloch's theorem says that the pressure field $p(x)$ has the same structure as the periodic potential $A(x)$, with K the Bloch wavenumber.

$$p(x) = A(x) \cdot e^{iKx} \qquad (1)$$

First, the effect of a single impedance jump for two different frequencies is discussed. Then the wave propagation for multiple, periodic impedance jumps, is described, again for two different frequencies. The impedance jumps are introduced by an instant change of the bulk density ρ from density ρ_1 to density ρ_2, as shown in Figure 3. A "forward" travelling wave from left to right is considered. At each impedance jump, the wave is partly reflected and the backwards travelling wave overlays with the incident wave.
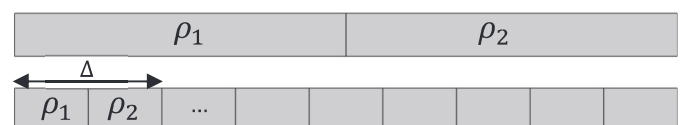

Figure 3: Single (upper) and periodic (lower) impedance jumps, introduced by instant change of the bulk density.

As depicted in Figure 4, in the case of a single impedance jump, the reflected wave interferes with the incident wave and the transmitted part travels further to the right but with lower amplitude. Because this effect is frequency independent, the amplitudes of the transmitted waves are identical. The transmission loss due to a single impedance jump introduced by a change in bulk density depends only on the ratio of the densities, where a higher ratio results in a higher impedance jump and a higher transmission loss.
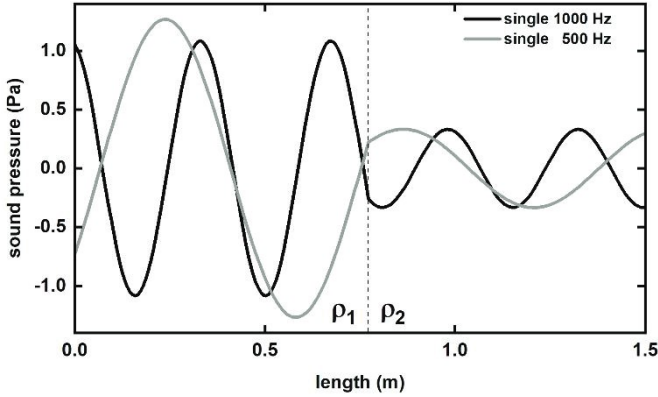

Figure 4: Sound pressure for two different frequencies along the waveguide with a single impedance jump, shown in the upper part of Figure 3.

However, as shown in Figure 5, in the case of multiple periodic impedance jumps the result of the interfering waves is strongly frequency dependent.
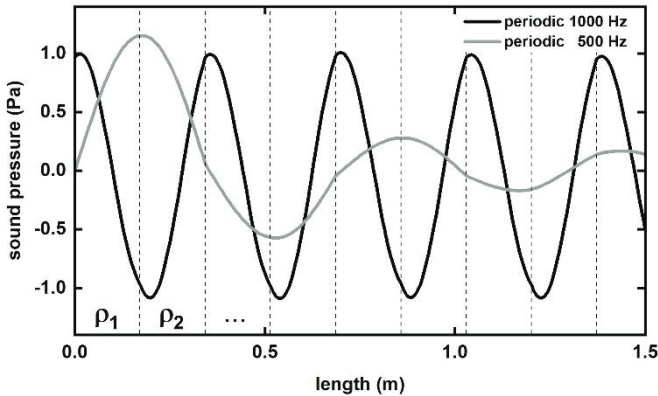

Figure 5: Sound pressure for two different frequencies along the waveguide with multiple periodic impedance jumps, shown in the lower part of Figure 3.

If the wavelength of the incident wave corresponds to an odd multiple of half the periodic spacing Δ, the amplitude along the waveguide decreases exponentially (500 Hz in Figure 5). This is the so-called "Bragg condition". If extended to infinity no wave propagation is possible in such a structure. Therefore, these frequency ranges are called "stopbands".

If the wavelength of the incident wave corresponds to an even multiple of half the periodic spacing Δ, the amplitude along the waveguide is constant (1000 Hz in Figure 5). Although the wave is partly reflected, the wave can propagate without

losses. This is because the reflections are in phase. Therefore, these frequency ranges are called "passbands".

Figure 6 shows this frequency-dependent property, where the transmission loss is plotted over the Helmholtz number defined as ratio of the periodic spacing over the wavelength.
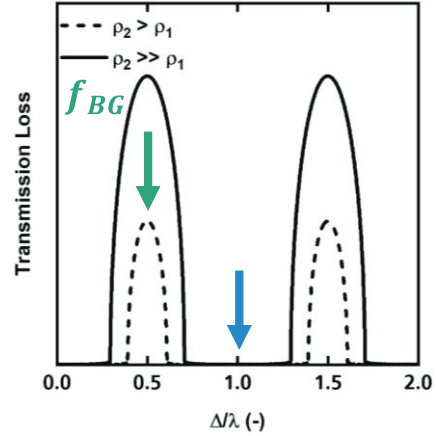

Figure 6: Transmission loss over the Helmholtz number.

The transmission loss is very high for some frequencies, for which the Bragg conditions are met (green arrow in Figure 6). The width and attenuation in these stopbands depends on the ratio between the two bulk densities. A higher ratio, e.g. higher jump in impedance, results in wider bands and higher attenuations. On the other hand, the transmission loss is close to zero for frequencies where the Bragg conditions are not met (blue arrow).

In the finite case, this transmission loss behaviour can be analysed analytically with the Transfer-Matrix-Method [1]. A one-dimensional waveguide can be modelled with a distributed element, given by equation 2, where l is the length of the waveguide, $Y = \rho_0 c_0 / S$ is the characteristic impedance and S is the surface area of the cross section.

$$\boldsymbol{T}_{distributed} = \begin{bmatrix} cos(kl) & jY\ sin(kl) \\ j/Y\ sin(kl) & cos(kl) \end{bmatrix} \qquad (2)$$

The entire finite waveguide is obtained by multiplying the individual elements, as given by equation 3.

$$\boldsymbol{T}_{finit} = \prod_{i=1}^{n} \boldsymbol{T}_i \qquad (3)$$

For a waveguide with a constant cross section, the transmission loss is given by equation 4.

$$TL = 20\ \lg \left| \frac{T_{11} + T_{12}/Y + T_{21} \cdot Y + T_{22}}{2} \right| \qquad (4)$$

In the infinitely periodic case, the band structure behaviour is analysed with the Bloch wave theory [2]. This analysis is based on the concept of the unit cell, the periodically repeating part of a structure with periodic boundary conditions.

The first step in the Transfer-Matrix-Method is the definition of the unit cell, given by equation 5.

$$T_{cell} = T_1 T_2 \tag{5}$$

The second step is the introduction of the periodic boundary conditions using Bloch's theorem (eq. 1), which leads to equation 6 and the eigenvalue problem, given by equation 7.

$$\begin{bmatrix} p_n \\ q_n \end{bmatrix} = T_{cell} \begin{bmatrix} p_{n+1} \\ q_{n+1} \end{bmatrix} = e^{iK\Delta} \begin{bmatrix} p_{n+1} \\ q_{n+1} \end{bmatrix} \tag{6}$$

$$\left| T_{cell} - e^{iK\Delta} \right| = 0 \tag{7}$$

The solution of the eigenvalue problem is given by equation 8 and is called the band structure.

$$cos(K\Delta) = \frac{1}{2}(T_{11} + T_{22}) \tag{8}$$

Figure 7 shows the band structure for the periodic impedance jumps (compare Figure 3). The results illustrate, that the stop bands occur at the odd multiples of the Bragg condition (green arrow), while the even multiples result in passbands (blue arrow). The left half of the diagram shows the imaginary part and the right half the real part of the normalized Bloch wavenumber. A stopband occurs if the imaginary part is non zero or the real part is constant.
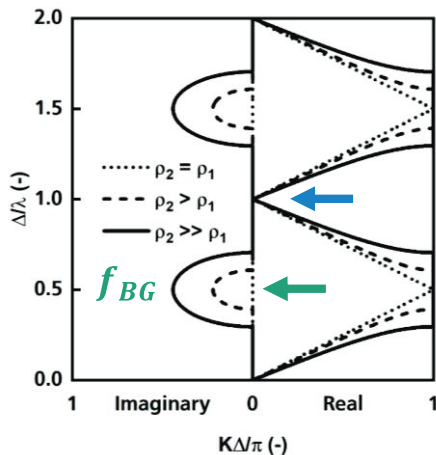

Figure 7: Band structure for the periodic impedance jumps, as shown in Figure 3.

The procedure of deriving the band structure in the finite element method (FEM) is similar to that in the Transfer-Matrix-Method [3]. As before, the first step is the definition of the unit cell. In the FEM, the geometry must be created and the material parameters must be defined. Then the periodic boundary conditions must be implemented, as shown in Figure 8.
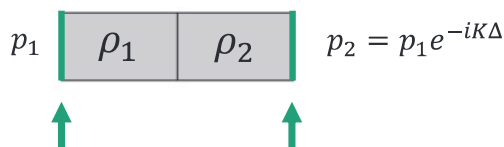

Figure 8: FEM model with periodic boundary conditions.

After that, an eigenfrequency analysis of the unit cell is conducted, which gives the Bloch modes. Plotting the eigenfrequencies over the Bloch wave number gives the band structure.

Figure 9 shows the comparison, between the band structure solution derived using the Transfer-Matrix-Method and the solution from the FE analysis of the periodic impedance jumps (compare Figure 3) are in good agreement.
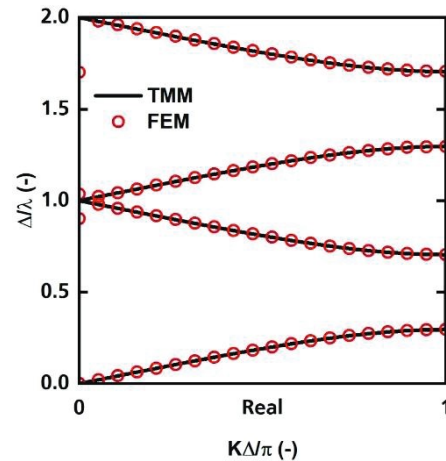

Figure 9: Comparison of the band structure solution from the TMM an FEM.

Experimental validation

Experimental studies have been conducted for validation. Instead of the periodically changing densities, the impedance jumps were generated using periodically arranged quarter wavelength resonators. The dimensions of the duct cross section are chosen such that the cut-on frequency is above the frequency range of interest. The length of the resonators and their periodic spacing are chosen such that the resonance frequency of the resonators and the Bragg frequency are identical. These parameters are chosen to create a stop band around 245 Hz. The dimensions are depicted in Figure 10.
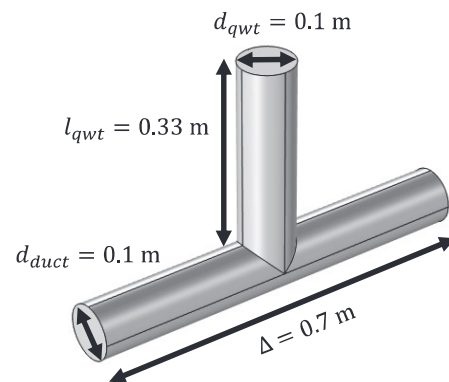

Figure 10: Unit cell with a quarter-wave resonator for the experimental validation.

The measurements were conducted on a silencer test bench according to ISO 7235 located in the DAkkS accredited laboratory at the Fraunhofer IBP in Stuttgart. Obviously, an experimental validation can only be performed for a finite resonator arrangement. Thus, an arrangement with seven resonators was chosen, as shown in Figure 11.

Figure 11: Test setup with seven quarter-wave resonator.

Figure 12 shows the measured and simulated transmission loss for the periodic arrangement of seven resonators in the frequency range between 100 Hz and 2000 Hz. The comparison shows a good agreement, especially for the first two stopbands. It should be noted that in the experimental results the maximum transmission loss in the first two stopbands is limited to a maximum of about 60 dB, which is the limiting transmission loss of the test bench. The comparison of the bandwidths of the measured stopbands with those of the predicted infinite stop bands (green shaded area) also shows reasonable good agreement at least for the first two stopbands. With increasing frequency the discrepancies between the experimental results and simulations increases. This is because the acoustic wavelength is decreasing with increasing frequency, and hence the absolute errors in the geometry of single resonators and the periodic spacing become increasingly important. This also means that Bragg conditions are not exactly matched at higher frequencies and the Bragg stop bands become defective.
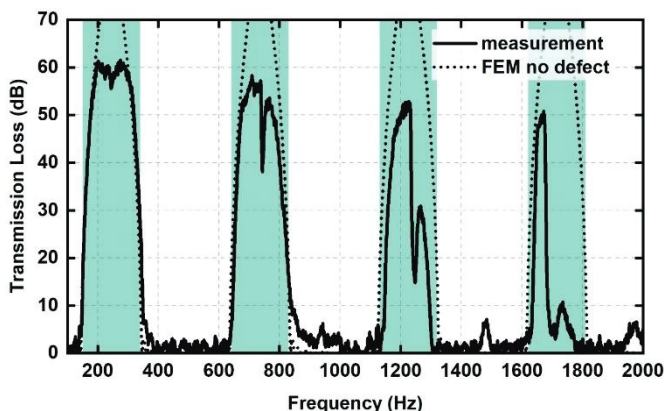

Figure 12: Comparison of measured and simulated transmission loss. Green shaded areas show the stopbands.

Outlook to further resonator concepts

The measurement results show that high transmission losses can be achieved with periodic resonator arrangements. The next question is how such an arrangement can be implemented in real ducts? One approach to construct acoustic resonators in a compact, space efficient way is that of a spiral resonator. Such a resonator for a round ventilation duct has been designed using the FEM. After the design was completed, an additive manufacturing process was used to fabricate the first prototype of the resonator, shown in Figure 13.
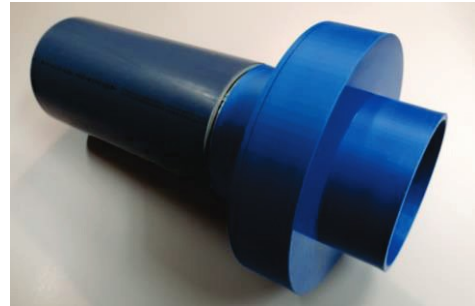

Figure 13: Prototype of a spiral resonator.

Additionally, the integration of active components has been studied with the aim to increase the acoustic performance of the resonator. For this, the spiral resonator is simulated with an integrated loudspeaker, and for different control concepts. The simulations show, that the resonance frequency can be tuned down to lower frequencies by more than one octave.
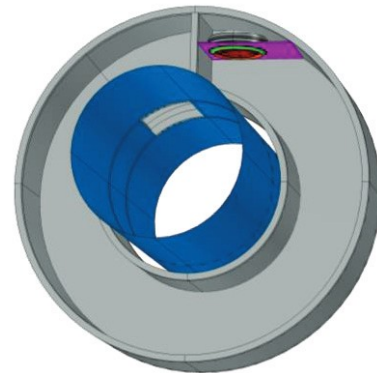

Figure 14: Spiral resonator with a loudspeaker as active component inside.

Acknowledgement

Literature

[1] Munjal, M. L.: Acoustics of Ducts and Mufflers. Wiley, Hoboken, 2014.

[2] Bradley, C. E.: Linear and Nonlinear Acoustic Bloch Wave Propagation in Periodic Waveguides, 1994.

[3] Yohko A., Seiji A., Maysenhölder, W.: Band Structure and Sound Transmission Loss of Infinite Periodic Partitions: Numerical Studies with COMSOL, DAGA 2018 München.